Journal of Sound and Vibration (1996) 000(0), 000–000

EXTENSION OF THE RECEPTANCE TECHNIQUE TO ACCOMMODATE DISTRIBUTED CONNECTIONS

B. K. GARDNER† AND J. S. BOLTON

1077 *Ray W. Herrick Laboratories, School of Mechanical Engineering, Purdue University, West Lafayette, IN* 47907-1077, *U.S.A.*

(*Received* 6 *September* 1995, *and in final form* 27 *February* 1996)

The receptance technique has been used most frequently to analyze the vibrational response of structures that may be idealized as a set of substructures connected at one or more discrete points. However, the receptance technique can also be used to analyze the response of structures connected along particular types of line junctions. In this paper, an extension to the receptance technique is presented that makes use of a generalized Fourier series approach to allow the evaluation of both the free and forced response of systems comprising components connected through spatially distributed junctions. The present extension is shown to reduce to the previous line receptance definition in the appropriate limit. The general distributed receptance formulation is demonstrated here through application to two problems involving coupled rods. The results obtained using the distributed receptance technique were found to compare well with the matching analytical solutions.

1. INTRODUCTION AND BACKGROUND

The receptance technique allows the dynamic response of a complex structure to be modelled through the systematic combination of component receptance models; i.e., the receptance of each component is found, and then they are linked together to form a global receptance matrix. By using the receptance model, both the free and forced response of a structure may be evaluated. A feature of the receptance method is that the individual component receptances may be found by different means; i.e., some of the receptances may be found analytically, some may be found by using finite element or other numerical methods, and some may be found by experiment. The application of the receptance technique to many simple elements is discussed by Bishop and Johnson [1] and its application to plates and shells is discussed by Soedel [2].

The receptance, α_{ij}, is defined as the displacement, u_i, at location i normalized by a harmonic force, f_j, applied at location j; i.e.,

$$\alpha_{ij} = u_i/f_j. \tag{1}$$

More precisely, the receptance can be written as

$$\alpha(\bar{x}_i,\bar{x}_j,\omega) = \frac{u(\bar{x}_i,\omega)|_{f@\bar{x}=\bar{x}_j}}{f(\bar{x}_j,\omega)}, \tag{2}$$

where $\bar{x}$ is the spatial co-ordinate vector and ω is the radian frequency of the harmonic excitation force. In general, a receptance may be considered to be a component transfer function that can be combined with other component receptances to generate system

0022–460X/96/000000 + 00 $18.00/0

response equations when they are coupled by using force and displacement compatability conditions. As originally proposed, each component is characterized by a set of receptance transfer functions that relate the forces and responses at a set of discrete locations; these methods are therefore particularly useful when applied to systems whose components are connected in a point-wise manner. In this paper, the receptance definition in equation (2) will be extended from a point-to-point receptance transfer function to a region-to-region receptance transfer function where a region may be a point, a line or a two-dimensional area. Region-to-region coupling allows the receptance technique to be used to analyze structures having any type of connection between their components.

The line connection was the first type of distributed connection that was considered in the context of the receptance method. Three types of line receptances will briefly be reviewed here.

When Wilken and Soedel [3,4] first applied the receptance method to plate and shell structures, the components of the systems they considered were required to be connected in a point-wise manner except in one case when a line connection was considered. They demonstrated that the spatial dependence of the receptance along a line connection could be eliminated from the system characteristic equation when the mode shapes of the unconnected components were identical along the line joining them. In that case it is possible to define a line receptance as

$$\alpha_{mm} = u_m/f_m, \tag{3}$$

where u_m is the coefficient of the mth mode of the displacement response and f_m is the mth coefficient of the expansion of the connection force in terms of the modal basis functions. By using this definition, the characteristic equation of the combined system may be found as if the line connected components were connected pointwise. Soedel and his colleagues have applied the concept of the line receptance to frame-stiffened, simply supported rectangular panels, ring-stiffened cylindrical shells [3,4], cylinders stiffened or terminated by circular plates, (e.g., end caps) [5,6], continuous rectangular plates [7], and cylindrical polygonal ducts [8,9]. Note that it is not possible to solve a forced response problem by using the receptance defined in equation (3), since it is a self-receptance, i.e., α_{mm}, and forced response problems require knowledge of transfer receptances.

The forced response of line connected systems can, however, be calculated by using the line transfer mobilities derived by Cuschieri [10] in the course of analyzing a problem involving the forced response of two coupled, flat plates. When re-formulated as a receptance, Cuschieri's line mobility becomes

$$\alpha_{mj} = u_m/f_j, \tag{4}$$

where u_m is the mth modal displacement in response to a point force, f_j, applied at location j.

Later, Huang and Soedel [11] defined a third line receptance. It is also a transfer receptance, and it relates the displacement at a point i, u_i, to the mth coefficient of the expansion of the connection force in terms of the modal basis functions, f_m; i.e.,

$$\alpha_{im} = u_i/f_m. \tag{5}$$

The transfer line receptances, equations (4) and (5), can be combined with the self line receptance, equation (3), to analyze either the free or forced response of structures featuring a combination of line and point connections. For example, Huang and Soedel applied all three types of line receptances to predict the forced response of a cylinder with a plate welded across each end [11].

It should be emphasized that the three line receptances defined above can only be used to couple components that have identical mode shapes along the line joining them.

Note also that when several component connections are involved, the "bookkeeping" required by the receptance technique can be tedious. To facilitate the manipulation and solution of the system equations, the receptance equations may be written in matrix form. As the number of components in the system increases, however, it becomes more and more awkward to couple the component receptance equations. The coupling involves application of the force and displacement compatability equations between each component. That coupling may be automated, however, by using the graph theory approach developed by Jetmundsen *et al.* [12] and later extended by Gordis *et al.* [13].

In addition to the receptance technique, other procedures have been developed that can accommodate distributed connections between components. Green function methods and the finite element method will next be discussed briefly.

Nicholson made use of a Green function to develop an integral formulation for the free response of line-stiffened plates [14]. However, since his approach is not receptance-based, it does not lend itself to a building block representation of multi-component structures. Nicholson used his approach to solve a number of example problems similar to those also considered by Soedel and his colleagues [3,4]. The complexity of the example problems was limited by the difficulty of deriving a Green's function for a plate having general boundary conditions.

Kelkel [15] has also discussed the use of a Green function approach to derive the receptance matrix for free–free rectangular plates that are stiffened by coupled beams. A large part of Kelkel's paper is devoted to deriving an approximate Green function and the associated point-connected receptance matrix for a free–free plate. The Green function involved a truncated triple summation and was obtained by analyzing four symmetric and antisymmetric problems. A complete analysis required the solution of four associated problems, each having carefully selected boundary conditions. This type of plate analysis is typical of the work of Gorman [16]. By coupling the plate Green function and the Green function of a beam with a Fourier series expansion of the shared displacements, Kelkel was able to derive the Green function, and then the receptance matrix, for a plate reinforced along a line by a coupled beam. Kelkel's method of coupling the beam and plate has been generalized in the present work to allow the development of a receptance for distributed connections.

The finite element method is very commonly used to model systems having distributed connections. The finite element method is usually based on stiffness equations rather than receptance equations, since it is easier to assemble the system equations for large numbers of components when using the stiffness matrix formulation. The two approaches can be related, however, since the dynamic stiffness matrix that appears in the finite element method, i.e., $[K - \omega^2 M]$, where K is the stiffness matrix, ω is the frequency in radians per second, and M is the mass matrix, is the inverse of the receptance matrix. If the terms in the dynamic stiffness matrix cannot be determined analytically, they can be measured, although with some difficulty. To measure D_{ij}, the displacement u_j resulting from a unit load applied at location i must be measured when all other external degrees of freedom are fixed. The stiffness measured in this way is usually called the "blocked" stiffness. Owing to the difficulty of experimentally fixing structural degrees of freedom, experimentally determined stiffnesses are rarely used to replace analytical stiffnesses. In addition, it is difficult to apply true point forces within the finite element method. A force applied at a node in a finite element representation does not represent a point force, but rather a distributed force the shape of which is described by a polynomial shape function.

Nonetheless, the finite element method remains the most commonly used technique for analyzing systems with distributed connections.

The Green function approach and the finite element method can both be used to couple extended components over a distributed region. In addition, several researchers have also made special provision to accommodate point-wise coupling between discrete and extended components in their analysis tools. For example, Hallquist and Snyder [17] considered the response of beams and plates coupled through point-connected viscous dampers. Recently, Tzioufas *et al.* [18] presented a method for coupling multiple point-connected discrete-distributed systems in the time domain. Particular attention was paid to a staged algorithm that could be used to solve the system eigenvalue problem. In addition, a technique called the Structural Analysis Method was developed by Pesterev and Tavrizov [19] to synthesize system models from the combination of distributed-finite structures interacting at a finite set of points. Their method makes use of Green functions to model the components and is described in terms of operator terminology. The major result of the Pesterev and Tavrizov Structural Analysis Method is the system receptance matrix (also called the Modal Force Matrix). The system eigenvalue problem is then solved by finding the frequencies at which the system receptance matrix is zero. Recall that even though the techniques described in this paragraph can be applied to mixed distributed-discrete systems, none of them can accommodate distributed connections; i.e., connections over a two-dimensional region.

From this survey of earlier work, it was concluded that the analysis procedures that can be used to represent distributed connections are as follows: line receptance analysis, the Green function approach and finite element analysis. Both the line receptance approach and finite element analysis provide modular, ready-to-use elements for synthesizing system equations. The Green function approach is flexible and may be applied to a great many problems, but it is not easily expressed in modular form, and analytical integration over the distributed connection region is usually required. Thus Green function methods do not have the same potential for the development of plug-in building blocks as do the line receptance and the finite element methods. The use of distributed receptances also appears to have several advantages when compared with the finite element method. In the finite element method, the solution is based on fitting a set of shape functions at every point of the system. In contrast, the use of the distributed receptance involves fitting a set of shape functions only over a distributed junction, a more economical procedure. In this resepct, the distributed receptance technique is similar to the boundary element method. In addition, since the concept of the distributed receptance may be easily used in combination with analytical solutions for component responses, discretization difficulties in optimization problems that occur when the finite element method is used [20,21] can be avoided. Also, true point sources and distributed loads of any type may both be modelled using the distributed receptance technique. Finally, note that when using the receptance technique, the system response is found by multiplying the system receptance matrix by the forcing vector (instead of by solving a matrix equation as in stiffness-based methods); thus the effect of each term in the receptance matrix on the system response is clear.

In summary, component synthesis methods are well developed in the context of receptance and stiffness approaches, have been presented in many variations and have been applied to many problems. However, when system components are joined over a distributed area, the finite element method is the only general purpose method currently available for analyzing the problem. For certain problems involving distributed connections, the line receptance method may be used while the Green function approach may be applied to other types of problems.

The present work entailed the extension of the receptance method to general distributed connections, thereby expanding the types of problems that may be addressed by using the receptance method.

2. DERIVATION OF RECEPTANCES WITH DISTRIBUTED CONNECTIONS

When extending the definition of a receptance to accommodate distributed connections between the individual components, it is convenient to start from the receptance definition, in equation (2), that can be rewritten as

$$u(\bar{x}_i,\omega)|_{f@\bar{x}=\bar{x}_j} = \alpha(\bar{x}_i,\bar{x}_j,\omega)f(\bar{x}_j,\omega). \tag{6}$$

A generalized Fourier series approach (see, for example, Churchill and Brown [22]) will be used here to extend the point-connection receptances to accommodate general distributed connections. An example system with a distributed connection is shown in Figure 1.

The displacement and force response terms in equation (6) need to be replaced by approximate forms when the contact is distributed over an area. The displacement, $u(\bar{x}_i,\omega)$ at location $\bar{x}_i$ is approximated as

$$u(\bar{x}_i,\omega) = \sum_{m=0}^{\infty} u_m(\omega)\phi_m(\bar{x}_i) \approx \sum_{m=0}^{N_i} u_m(\omega)\phi_m(\bar{x}_i) \approx \bar{\phi}(\bar{x}_i)^{\mathrm{T}}\bar{u}(\omega), \tag{7}$$

and the force $f(\bar{x}_j,\omega)$ at location $\bar{x}_j$ is approximated as

$$f(\bar{x}_j,\omega) = \sum_{n=0}^{\infty} f_n(\omega)\psi_n(\bar{x}_j) \approx \sum_{n=0}^{N_j} f_n(\omega)\psi_n(\bar{x}_j) \approx \bar{\psi}(\bar{x}_j)^{\mathrm{T}}\bar{f}(\omega), \tag{8}$$

where the $\phi_m(\bar{x}_i)$'s are a set of shape functions used to describe the displacement over area i, and the $\psi_n(\bar{x}_j)$'s are a set of shape functions used to describe the force over area j. The displacement shape function contribution coefficients, $\bar{u}(\omega)$, are given by

$$\bar{u}(\omega) = \left[\int\!\!\int_{A_i} \bar{\phi}(\bar{x}_i)\bar{\phi}(\bar{x}_i)^{\mathrm{T}}\mathrm{d}A_i\right]^{-1}\left\{\int\!\!\int_{A_i} \bar{\phi}(\bar{x}_i)u(\bar{x}_i,\omega)\mathrm{d}A_i\right\}, \tag{9}$$

but if the displacement shape functions, $\phi(\bar{x}_i)$, are orthonormal, the matrix in equation (9) reduces to the identity matrix, and the mth shape function coefficient, $u_m(\omega)$, is simply

$$u_m(\omega) = \int_{A_i} \phi_m(\bar{x}_i)u(\bar{x}_i,\omega)\mathrm{d}A_i. \tag{10}$$

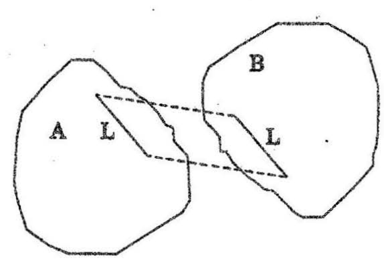

Figure 1. Subcomponents A and B joined along line L.

The force shape function contribution coefficients, $\bar{f}(\omega)$, may be defined in a similar manner. The shape functions may be selected from any set of complete functions. However, in regions that will be connected in the combined structure, the same shape functions must be used in both components.

When multiple point forces drive the system, equation (6) becomes

$$u(\bar{x}_i,\omega)|_{f@\{\bar{x}_j j=1,\ldots,N_j\}} = \sum_{j=1}^{N_j} \alpha(\bar{x}_i,\bar{x}_j,\omega) f_j(\bar{x}_j,\omega). \tag{11}$$

The response due to a distributed force may be found by approximating the distributed force as a large number of point forces. As the number of point forces, N_j, goes to infinity, the summation in equation (11) may be replaced by an integral, to give

$$u(\bar{x}_i,\omega)|_{f@\{\bar{x}_j\in A_j\}} = \int_{A_j} \alpha(\bar{x}_i,\bar{x}_j,\omega) f(\bar{x}_j,\omega)\,\mathrm{d}A_j. \tag{12}$$

The distributed force, $f(\bar{x}_j,\omega)$, in equation (12), may be approximated by using equation (8) to give

$$u(\bar{x}_i,\omega)|_{f@\{\bar{x}_j\in A_j\}} = \left\{\int_{A_j} \alpha(\bar{x}_i,\bar{x}_j,\omega)\bar{\psi}(\bar{x}_j)^{\mathrm{T}}\,\mathrm{d}A_j\right\}\bar{f}(\omega). \tag{13}$$

From equation (13) the generalized receptance vector that relates the displacement spectrum at a point to the force shape function contribution coefficients, $\bar{f}(\omega)$, is given by

$$\bar{\alpha}_{g_{iA_j}}(\omega) = \left\{\int_{A_j} \alpha(\bar{x}_i,\bar{x}_j,\omega)\bar{\psi}(\bar{x}_j)\,\mathrm{d}A_j\right\}. \tag{14}$$

The receptance that relates the force over an area, A_j, to the displacement over another area, A_i, may be obtained by extending equation (13) to account for a distributed response. This can be done by taking equation (9) (that defines the displacement shape function participation factors in terms of the displacement field) and substituting it into equation (13) as a definition of the displacement field. That operation results in

$$\bar{u}(\omega) = \left[\int_{A_i} \bar{\phi}(\bar{x}_i)\bar{\phi}(\bar{x}_i)^{\mathrm{T}}\,\mathrm{d}A_i\right]^{-1}\left[\int_{A_i}\int_{A_j} \alpha(\bar{x}_i,\bar{x}_j,\omega)\bar{\phi}(\bar{x}_i)\bar{\psi}(\bar{x}_j)^{\mathrm{T}}\,\mathrm{d}A_j\,\mathrm{d}A_i\right]\bar{f}(\omega). \tag{15}$$

The receptance matrix that relates the force shape function participation factors to the displacement shape function participation factors is then

$$[\alpha_{g_{A_iA_j}}(\omega)] = \left[\int_{A_i} \bar{\phi}(\bar{x}_i)\bar{\phi}(\bar{x}_i)^{\mathrm{T}}\,\mathrm{d}A_i\right]^{-1}\left[\int_{A_i}\int_{A_j} \alpha(\bar{x}_i,\bar{x}_j,\omega)\bar{\phi}(\bar{x}_i)\bar{\psi}(\bar{x}_j)^{\mathrm{T}}\,\mathrm{d}A_j\,\mathrm{d}A_i\right]. \tag{16}$$

A special case of the receptance that relates a force over a distributed region to a displacement over a distributed region is the case in which the force and displacement are both distributed over the same region. In this case the receptance is

$$[\alpha_{g_{A_iA_i}}(\omega)] = \left[\int_{A_i} \bar{\phi}(\bar{x}_i)\bar{\phi}(\bar{x}_i)^{\mathrm{T}}\,\mathrm{d}A_i\right]^{-1}\left[\int_{A_i}\int_{A_i} \alpha(\bar{x}_i,\bar{x}_i,\omega)\bar{\phi}(\bar{x}_i)\bar{\phi}(\bar{x}_i)^{\mathrm{T}}\,\mathrm{d}A_i\,\mathrm{d}A_i\right]. \tag{17}$$

The receptance that relates a point force to a distributed field may be obtained by substituting equation (6) into equation (9), which results in

$$\bar{u}(\omega)=\left[\int_{A_i}\bar{\phi}(\bar{x}_i)\bar{\phi}(\bar{x}_i)^{\mathrm{T}}\mathrm{d}A_i\right]^{-1}\left[\int_{A_i}\alpha(\bar{x}_i,\bar{x}_j,\omega)\bar{\phi}(\bar{x}_i)\mathrm{d}A_i\right]f(\bar{x}_j,\omega). \qquad (18)$$

The receptance vector that relates a point force to the displacement shape function participation coefficient vector is then

$$\bar{\alpha}_{g_{A_iA_j}}(\omega)=\left[\int_{A_i}\bar{\phi}(\bar{x}_i)\bar{\phi}(\bar{x}_i)^{\mathrm{T}}\mathrm{d}A_i\right]^{-1}\left[\int_{A_i}\alpha(\bar{x}_i,\bar{x}_j,\omega)\bar{\phi}(\bar{x}_i)\mathrm{d}A_i\right]. \qquad (19)$$

The distributed receptances that were developed in this section may be used in the same way as standard point receptances; i.e., to derive the characteristic equation, mode shapes and forced response of the system. In the case in which subcomponent α is joined to subcomponent β at the distributed region i, the force and displacement over region i on subcomponent α are approximated by

$$u^{\alpha_i}(\bar{x}_i,\omega)=\bar{\phi}(\bar{x}_i)^{\mathrm{T}}\bar{u}^{\alpha_i}(\omega) \qquad (20)$$

and

$$f^{\alpha_i}(\bar{x}_i,\omega)=\bar{\phi}(\bar{x}_i)^{\mathrm{T}}\bar{f}^{\alpha_i}(\omega), \qquad (21)$$

respectively. The force and displacement over region i on subcomponent β are approximated by

$$u^{\alpha_i}(\bar{x}_i,\omega)=\bar{\phi}(\bar{x}_i)^{\mathrm{T}}\bar{u}^{\beta_i}(\omega) \qquad (22)$$

and

$$f^{\alpha_i}(\bar{x}_i,\omega)=\bar{\phi}(\bar{x}_i)^{\mathrm{T}}\bar{f}^{\beta_i}(\omega), \qquad (23)$$

respectively. Any externally applied load in region i is approximated by

$$f^{ext_i}(\bar{x}_i,\omega)=\bar{\phi}(\bar{x}_i)^{\mathrm{T}}\bar{f}^{ext_i}(\omega). \qquad (24)$$

The compatibility equations then become equations in terms of the unknown shape function coefficients. The compatibility equations to be satisfied over region i are the continuity of displacement,

$$\bar{u}^{\alpha_i}(\omega)=\bar{u}^{\beta_i}(\omega), \qquad (25)$$

and the force balance,

$$\bar{f}^{\alpha_i}(\omega)+\bar{f}^{\beta_i}(\omega)=\bar{f}^{ext_i}(\omega). \qquad (26)$$

The equations developed in this section provide a formalism for applying the receptance method to systems having distributed connections. The extended definition of the receptance has been developed so that problems featuring distributed connections can be solved in a manner similar to problems featuring point connections.

3. DISTRIBUTED RECEPTANCES FOR COMPONENTS DEFINED BY MODAL PARAMETERS

The displacement, u, of any linear, elastic structure can be modelled by using a linear partial differential equation (or by using a set of linear partial differential equations) that has the form

$$\mathscr{L}\{u_t\} - \lambda \dot{u}_t - m\ddot{u}_t = -q_t, \tag{27}$$

where $\mathscr{L}$ is a linear stiffness operator, λ is the equivalent viscous damping factor, m is a mass term (usually mass per unit length or mass per unit area), q is the force applied to the system and the subscript t denotes a time-dependent variable. When a harmonic time dependence of the form, $u_t = u\mathrm{e}^{\mathrm{j}\omega t}$, is assumed, equation (27) becomes

$$\mathscr{L}\{u\} - \mathrm{j}\omega\lambda u + m\omega^2 u = -q. \tag{28}$$

After applying boundary conditions to equation (28), the eigenvalue problem can be solved. (Note that when calculating the receptance of a component that will be combined with other components to calculate a system response, the boundary conditions should be those that are present when the component is disconnected from the rest of the system.) The eigenvalues are the natural frequencies, ω_k, and the eigenvectors are the mode shapes, $U_k(\bar{x})$. The displacement is then given by

$$u(\bar{x},\omega) = \sum_{k=1}^{\infty} \frac{Q_k U_k(\bar{x})}{\omega_k^2 - \omega^2 + 2\mathrm{j}\zeta_k\omega_k\omega} \approx \sum_{k=1}^{N_k} \frac{Q_k U_k(\bar{x})}{\omega_k^2 - \omega^2 + 2\mathrm{j}\zeta_k\omega_k\omega}, \tag{29}$$

where

$$\zeta_k = \lambda/2m\omega_k \tag{30}$$

is the modal damping coefficient and

$$Q_k = \frac{\int_A qU_k(\bar{x})\mathrm{d}A}{m\int_A U_k^2(\bar{x})\mathrm{d}A} \tag{31}$$

is the modal forcing function. In equation (31), the integral is over the entire component, region A, as defined in Figure 1.

3.1. RESPONSE TO A POINT FORCE

When the force, q, is a point force acting at location, j, i.e.,

$$q = f_j(\omega)\delta(\bar{x}_j), \tag{32}$$

the modal forcing function is

$$Q_k = \frac{\int_A f_j(\omega)\delta(\bar{x}_j)U_k(\bar{x})\mathrm{d}A}{m\int_A U_k^2(\bar{x})\mathrm{d}A} = \frac{f_j(\omega)U_k(\bar{x}_j)}{m\int_A U_k^2(\bar{x})\mathrm{d}A}. \tag{33}$$

The corresponding displacement response is

$$u(\bar{x},\omega) = \sum_{k=1}^{N_k} \frac{U_k(\bar{x}_j)U_k(\bar{x})}{m(\omega_k^2 - \omega^2 + 2j\zeta_k\omega_k\omega)\left(\int_A U_k^2 \mathrm{d}A\right)} f_j(\omega) \tag{34}$$

and thus the receptance for a system described in terms of modal parameters is

$$\alpha(\bar{x}_i,\bar{x}_j,\omega) = \sum_{k=1}^{N_k} \frac{U_k(\bar{x}_i)U_k(\bar{x}_j)}{m(\omega_k^2 - \omega^2 + 2j\zeta_k\omega_k\omega)\left(\int_A U_k^2 \mathrm{d}A\right)}. \tag{35}$$

3.2. RESPONSE TO A DISTRIBUTED FORCE

When the force, q, is a distributed force acting over region, j, as expressed by

$$q = f_j(\bar{x}_j,\omega) \approx \bar{\psi}(\bar{x})^{\mathrm{T}}\bar{f}(\omega)\mathscr{U}(\bar{x},A_j), \tag{36}$$

where $\mathscr{U}$ is a unit step function defined as

$$\mathscr{U}(\bar{x},A) = \begin{cases} 1, & \bar{x}\in A, \\ 0, & \text{otherwise}, \end{cases} \tag{37}$$

the modal forcing funtion is

$$Q_k = \frac{\int_A \bar{\psi}(\bar{x})^{\mathrm{T}}\bar{f}(\omega)U_k(\bar{x})\mathscr{U}(\bar{x},A_j)\mathrm{d}A}{m\int_A U_k^2(\bar{x})\mathrm{d}A} = \frac{\int_{A_j} \bar{\psi}(\bar{x}_j)^{\mathrm{T}}U_k(\bar{x}_j)\mathrm{d}A_j}{m\int_A U_k^2(\bar{x})\mathrm{d}A}\bar{f}(\omega). \tag{38}$$

The corresponding displacement response is

$$u(\bar{x},\omega) = \sum_{k=1}^{N_k} \frac{\left\{\int_{A_j} \bar{\psi}(\bar{x}_j)^{\mathrm{T}}U_k(\bar{x}_j)\mathrm{d}A_j\right\}U_k(\bar{x})}{m(\omega_k^2 - \omega^2 + 2j\zeta_k\omega_k\omega)\left(\int_A U_k^2 \mathrm{d}A\right)}\bar{f}(\omega). \tag{39}$$

3.3. CALCULATION OF THE DISTRIBUTED RECEPTANCES FROM MODAL POINT-TO-POINT RECEPTANCES

The modal form of the point-to-point receptance in equation (35) may be substituted into equations (14), (19) and (16) to give the modal forms of the three distributed receptances. The generalized receptance that relates a distributed force to a point displacement is found to be

$$\bar{\alpha}_{g_i A_j}(\omega) = \left\{\sum_{k=1}^{N_k} \frac{U_k(\bar{x}_i)\int_{A_j}U_k(\bar{x}_j)\bar{\psi}(\bar{x}_j)\mathrm{d}A_j}{m(\omega_k^2 - \omega^2 + 2j\zeta_k\omega_k\omega)\left(\int_A U_k^2 \mathrm{d}A\right)}\right\}. \tag{40}$$

The generalized receptance that relates a point force to a distributed displacement is

$$\bar{\alpha}_{g_{A_{ij}}}(\omega) = \left[\int_{A_i} \bar{\phi}(\bar{x}_i)\bar{\phi}(\bar{x}_i)^{\mathrm{T}}\mathrm{d}A_i\right]^{-1} \sum_{k=1}^{N_k} \frac{\int_{A_i} U_k(\bar{x}_i)\bar{\phi}(\bar{x}_i)\mathrm{d}A_i U_k(\bar{x}_j)}{m(\omega_k^2 - \omega^2 + 2\mathrm{j}\zeta_k\omega_k\omega)\left(\int_A U_k^2 \mathrm{d}A\right)} \quad (41)$$

and the generalized receptance that relates a distributed force to a distributed displacement is

$$[\alpha_{g_{A_iA_j}}(\omega)] = \left[\int_{A_i} \bar{\phi}(\bar{x}_i)\bar{\phi}(\bar{x}_i)^{\mathrm{T}}\mathrm{d}A_i\right]^{-1}$$

$$\times \sum_{k=1}^{N_k} \frac{\left\{\int_{A_i} U_k(\bar{x}_i)\bar{\phi}(\bar{x}_i)\mathrm{d}A_i\right\}\left\{\int_{A_j} U_k(\bar{x}_j)\bar{\psi}(\bar{x}_j)\mathrm{d}A_j\right\}^{\mathrm{T}}}{m(\omega_k^2 - \omega^2 + 2\mathrm{j}\zeta_k\omega_k\omega)\left(\int_A U_k^2 \mathrm{d}A\right)}. \quad (42)$$

3.4. CALCULATION OF THE DISPLACEMENT DUE TO A DISTRIBUTED FORCE USING THE GENERALIZED RECEPTANCE

Equation (40) can be used to calculate the displacement at a point, x_i, as

$$u(\bar{x}_i,\omega)|_{f@\bar{x}=\bar{x}_i} = \{\bar{\alpha}_{iA_j}(\omega)\}^{\mathrm{T}}\bar{f}. \quad (43)$$

Thus the displacement at location x_i is

$$u(\bar{x}_i,\omega) = \sum_{k=1}^{N_k} \frac{U_k(\bar{x}_i)\int_{A_j} U_k(\bar{x}_j)\bar{\psi}(\bar{x}_j)\mathrm{d}A_j}{m(\omega_k^2 - \omega^2 + 2\mathrm{j}\zeta_k\omega_k\omega)\left(\int_A U_k^2 \mathrm{d}A\right)}^{\mathrm{T}} \bar{f}. \quad (44)$$

Note that equation (44) is the same as the displacement calculated using direct modal expansion when the structure is excited by a distributed force of the form, $\bar{f}(\omega) = \bar{\psi}(\bar{x})^{\mathrm{T}}\bar{f}(\omega)$, as in equation (39), thereby validating the generalized receptance that relates a distributed force to a point displacement (equation (40)).

4. SHAPE FUNCTION SELECTION

Up to this point, the shape functions, ϕ and ψ, have not been specified, except that any shape functions that represent a function over the same region of the combined structure must be identical over that region. Also, it was implied that $\bar{\phi}(\bar{x}_i)^{\mathrm{T}}\bar{u}(\omega)$ was an acceptable approximation of $f(\bar{x}_j,\omega)$. Many different shape functions will satisfy these criteria. In this section, specific shape functions or classes of potential shape functions will be considered.

4.1. ORTHONORMAL SHAPE FUNCTIONS

When the shape functions that are used to approximate the displacement, $\bar{\phi}(\omega)$, are orthonormal over the region i, then the matrix $[\int_{A_i}\bar{\phi}(\bar{x}_i)\bar{\phi}(\bar{x}_i)^{\mathrm{T}}\mathrm{d}A_i]$ becomes the identity matrix and its inverse can be removed from all the definitions of the receptance matrices in which it appears. In general, that is the only simplification that follows from using orthonormal shape functions.

4.2. MODAL SHAPE FUNCTIONS

In the case in which a modal description is used to specify the point-to-point receptances, it may be advantageous to select shape functions that are the same as the modes of one of the components over the region i or j. In general, no simplification results from selecting the shape functions to coincide with the modes. However, the approximations to the displacement and force fields should provide better results with fewer terms in the series when the shape functions are made up of the characteristic shapes of the subsystem.

If the modal shape functions happen to be orthogonal over the distributed contact region, then the form of the distributed receptances will be simplified. Selection of the modal functions as the shape functions gives

$$\bar{\psi}(\bar{x}_j) = \bar{U}(\bar{x}_j) \tag{45}$$

and

$$\bar{\phi}(\bar{x}_i) = \bar{U}(\bar{x}_i). \tag{46}$$

As an example of the modal receptance, equation (40) becomes

$$\bar{\alpha}_{g_{i,A_j}}(\omega) = \sum_{k=1}^{N_k} \frac{U_k(\bar{x}_i)\displaystyle\int_{A_j} U_k(\bar{x}_j)\bar{U}(\bar{x}_j)\mathrm{d}A_j}{m(\omega_k^2 - \omega^2 + 2\mathrm{j}\zeta_k\omega_k\omega)\left(\displaystyle\int_A U_k^2\mathrm{d}A\right)} \tag{47}$$

when the modal shape function, equation (45), is used. If the modes are orthonormal over the entire subcomponent, then

$$\int_A U_k^2\mathrm{d}A = 1. \tag{48}$$

If the modes are orthogonal over the contact region, then

$$\int_{A_j} U_k(\bar{x}_j)\bar{U}(x_j)\mathrm{d}A_j = U_k' EL_k, \tag{49}$$

where EL_k is the elementary vector with all-zero elements, except for the kth element which is unity, and

$$U_k' = \int_{A_j} U_k(\bar{x}_j)U_k(\bar{x}_j)\mathrm{d}A_j. \tag{50}$$

There is also an elementary matrix, EL_{ij}, which contains all-zero elements except for the ijth element, which is unity. When the orthogonality condition is met (equation (49)), the kth element of equation (47) reduces to

$$\alpha_{g_{iA_j}}^{(k)}(\omega) = \frac{U_k(\bar{x}_i)U_k'}{m(\omega_k^2 - \omega^2 + 2j\zeta_k\omega_k\omega)\left(\int_A U_k^2 \mathrm{d}A\right)}. \tag{51}$$

Over region i, the kth element of equation (41) becomes

$$\alpha_{g_{A_{ij}}}^{(k)}(\omega) = \frac{U_k' U_k(\bar{x}_j)}{m(\omega_k^2 - \omega^2 + 2j\zeta_k\omega_k\omega)\left(\int_A U_k^2 \mathrm{d}A\right)} \tag{52}$$

and when regions i and j coincide, equation (42) becomes a diagonal matrix in which

$$\alpha_{g_{A_iA_j}}^{(k)}(\omega) = \frac{U_k'^2}{m(\omega_k^2 - \omega^2 + 2j\zeta_k\omega_k\omega)\left(\int_A U_k^2 \mathrm{d}A\right)} \tag{53}$$

is the kth diagonal term.

The more common case is the one in which the shape function is the same as a portion of the mode shape, and is orthogonal to a portion of the modal shape functions. In this case, the mode shape function, $U_k(\bar{x}_j)$, can be rewritten as

$$U_k(\bar{x}_j) = U_{mn}(\bar{x}_j) = U_m'(\bar{x}_j')U_n''(\bar{x}_j'') \tag{54}$$

where the k modal index has been reparameterized into an m and n pair of modal indices, the spatial co-ordinates, $\bar{x}_j$, have been split into two sets of co-ordinates, $\bar{x}_j'$ and $\bar{x}_j''$ (typically these are now each a single co-ordinate, but in general they are vectors), and the modal shape function has been split into two parts which correspond to the new co-ordinate definition. The m and n indices also correspond to the new split co-ordinate definition. Selection of the shape functions to be the second part of the modal functions (that is, the part that varies over the contact region) gives

$$\psi_n(\bar{x}_j'') = U_n''(\bar{x}_j'') \tag{55}$$

and

$$\phi_n(\bar{x}_i'') = U_n''(\bar{x}_i'') \tag{56}$$

The modal receptance that relates a distributed force to a point displacement, equation (40), for this second class of modal shape functions becomes

$$\bar{\alpha}_{g_{iA_j}}(\omega) = \sum_{m=1}^{N_m}\sum_{n=1}^{N_n} \frac{U_{mn}(\bar{x}_i)\int_{A_j} U_m'(\bar{x}_j')U_n''(\bar{x}_j'')\bar{U}''(\bar{x}_j'')\mathrm{d}\bar{x}_j''}{m(\omega_{mn}^2 - \omega^2 + 2j\zeta_{mn}\omega_{mn}\omega)\left(\int_A U_{mn}^2 \mathrm{d}A\right)} \tag{57}$$

when the modal shape function, equation (55), is used. The orthogonality condition over the contact region is

$$\int_{A_j} U_n''(\bar{x}_j'')\bar{U}''(\bar{x}_j'')\mathrm{d}\bar{x}_j'' = U_n'''EL_n, \tag{58}$$

where EL_k is the elementary vector and

$$U_n''' = \int_{A_j} U_n''(\bar{x}_j'')^2\mathrm{d}\bar{x}_j''. \tag{59}$$

When the orthogonality condition is met (equation (58)), the summation over n sums N_n orthogonal vectors which reduce to a single vector. The nth element of the distributed receptance $\bar{\alpha}_{g_{iA_j}}(\omega)$ in equation (57) becomes

$$\alpha_{g_{iA_j}}^{(n)}(\omega) = \sum_{m=1}^{N_m} \frac{U_{mn}(\bar{x}_i)U_m'(\bar{x}_j')U_n'''}{m(\omega_{mn}^2 - \omega^2 + 2\mathrm{j}\zeta_{mn}\omega_{mn}\omega)\left(\int_A U_{mn}^2\mathrm{d}A\right)}. \tag{60}$$

In the case of the receptance that relates a point force to a distributed displacement, the mode shape function, $U_k(\bar{x}_j)$, can be rewritten as

$$U_k(\bar{x}_i) = U_{mn}(\bar{x}_i) = U_m'(\bar{x}_i')U_n''(\bar{x}_i''). \tag{61}$$

Substitution of the mode shape function, equation (61), and the displacement shape function, equation (56), into equation (41) gives

$$\bar{\alpha}_{g_{A_ij}}(\omega) = \left\{\left[\int_{A_i} \bar{U}''(\bar{x}_i'')\bar{U}''(\bar{x}_i'')^{\mathrm{T}}\mathrm{d}\bar{x}_i''\right]^{-1}\right.$$

$$\left.\times \sum_{m=1}^{N_m}\sum_{n=1}^{N_n} \frac{\int_{A_i} U_m'(\bar{x}_i')U_n''(\bar{x}_i'')\bar{U}''(\bar{x}_i'')\mathrm{d}\bar{x}_i''U_{mn}(\bar{x}_j)}{m(\omega_{mn}^2 - \omega^2 + 2\mathrm{j}\zeta_{mn}\omega_{mn}\omega)\left(\int_A U_{mn}^2\mathrm{d}A\right)}\right\}. \tag{62}$$

Then, application of the orthogonality condition (which is the same as equation (58), except that j is now replaced with i) to equation (62) gives

$$\alpha_{g_{A_ij}}^{(n)}(\omega) = \sum_{m=1}^{N_m}\left\{\frac{U_m'(\bar{x}_i')U_{mn}(\bar{x}_j)}{m(\omega_{mn}^2 - \omega^2 + 2\mathrm{j}\zeta_{mn}\omega_{mn}\omega)\left(\int_A U_{mn}^2\mathrm{d}A\right)}\right\} \tag{63}$$

for the nth element of $\bar{\alpha}_{g_{A_ij}}(\omega)$.

When distributed regions i and j coincide, and upon substitution of equation (54) for the mode shape, equations (55) and (56) for the shape functions, and the replacement of j with i, equation (42) becomes

$$[\alpha_{g_{A_iA_i}}(\omega)] = [\Phi_i]^{-1}\sum_{m=1}^{N_m}\sum_{n=1}^{N_n}\frac{\bar{\phi}_i'\bar{\phi}_i'^{\mathrm{T}}}{m(\omega_{mn}^2-\omega^2+2\mathrm{j}\zeta_{mn}\omega_{mn}\omega)\left(\int_A U_{mn}^2\,\mathrm{d}A\right)}, \tag{64}$$

where

$$[\Phi_i] = \int_{A_i} \bar{U}''(\bar{x}_i'')\bar{U}''(\bar{x}_i'')^{\mathrm{T}}\,\mathrm{d}\bar{x}_i'' \tag{65}$$

and

$$\bar{\phi}_i' = \int_{A_i} U_m'(\bar{x}_i')U_n''(\bar{x}_i'')\bar{U}''(\bar{x}_i'')\,\mathrm{d}\bar{x}_i''. \tag{66}$$

After applying the orthogonality conditions expressed in equations (58) and (59), equation (64) becomes a diagonal matrix in which

$$\alpha_{g_{A_iA_i}}^{(n)}(\omega) = \sum_{m=1}^{N_m}\left\{\frac{U_m'(\bar{x}_i')^2U_n'''}{m(\omega_k^2-\omega^2+2\mathrm{j}\zeta_{mn}\omega_{mn}\omega)\left(\int_A U_{mn}^2\,\mathrm{d}A\right)}\right\} \tag{67}$$

is the nth diagonal term.

5. COMPARISON WITH LINE RECEPTANCES

As mentioned in the opening section of this paper, the line receptance technique has been applied to a variety of problems in which the joining substructures had identical mode shapes over the line connection and the mode shapes were orthogonal over the line connection [2,3,5,6,11]. In this section, a general presentation of the line receptance as it is used for free response problems will be developed. The modal distributed receptance definition with the appropriate modal characteristics, equation (53), will be evaluated for a line connection. The distributed receptance formulation will be shown to be identical to the line receptance formulation when applied to a problem in which the line receptance can be used.

The geometry of a general line receptance connection is shown in Figure 1. The mnth mode shape of component A is defined as

$$U_{A_{mn}}(\bar{x}) = U_{L_n}(\bar{x}_L)U_{A_m}'(\bar{x}') \tag{68}$$

and the mnth mode shape of component B is defined as

$$U_{B_{mn}}(\bar{x}) = U_{L_n}(\bar{x}_L)U_{B_m}'(\bar{x}'), \tag{69}$$

where $\bar{x}_L$ is the co-ordinate along the connecting line, the co-ordinate vector, $\bar{x}'$, contains all of the co-ordinates except $\bar{x}$, $U_{L_n}(\bar{x}_L)$ is the nth mode shape along the line connection, $U_{A_m}'(\bar{x}')$ is the part of the mode shape of subcomponent A that is not along the line connection, and $U'_{B_{m}}(\bar{x}')$ is the part of the mode shape of subcomponent B that is not along the line connection.

First, assume that the forcing function along the line connection is of the form

$$f_{L_p}(x_L,\omega) = F(\omega)U_{L_p}(x_L). \tag{70}$$

Then the displacement response at location $\bar{x}_i$ on subcomponent A is

$$U(\bar{x}_i,\omega) = \sum_{m=1}^{N_m}\sum_{n=1}^{N_n} \frac{F_{mn}(\omega)U_{L_n}(x_{L_j})U_{A_m}(\bar{x}_i')}{m_A(\omega^2_{A_{mn}} - \omega^2 + 2j\zeta_{A_{mn}}\omega_{A_{mn}}\omega)\left(\int_{A_A} U^2_{mn}\,\mathrm{d}A\right)}. \tag{71}$$

where $F_{mn}(\omega)$ is

$$F_{mn}(\omega) = \iint_{A_A} (f_{L_p}(x_L,\omega)\delta(\bar{x}' - \bar{x}_L'))(U_{L_n}(\bar{x}_L)U'_{A_m}(\bar{x}'))\mathrm{d}x_L\,\mathrm{d}\bar{x}' \tag{72}$$

$$= F(\omega)U_{A_m}(\bar{x}_L')\int_L U_{L_p}(\bar{x}_L)U_{L_n}(\bar{x}_L)\mathrm{d}x_L \tag{73}$$

and $\bar{x}_L'$ is the location of the line. Because the mode shapes are orthogonal along the line, the final form of the modal force participation factor is

$$F_{mn}(\omega) = \begin{cases} F(\omega)U_{Am}(\bar{x}_L')U'_{L_n} & \text{for}\, n = p, \\ 0 & \text{for}\, n \neq p, \end{cases} \tag{74}$$

where

$$U'_{L_n} = \int_L U_{L_n}(\bar{x}_L)^2\mathrm{d}x_L. \tag{75}$$

The receptance, $\alpha_p(\bar{x}_i,L,\omega)$, is defined as

$$\alpha_p(\bar{x}_i,L,\omega) = \frac{u(\bar{x}_i,\omega)}{f_{L_p}(x_L,\omega)} \tag{76}$$

or

$$\alpha_p(\bar{x}_i,L,\omega) = \frac{1}{U_{L_p}(x_L)}\sum_{m=1}^{N_m}\left[\frac{U_{A_m}(\bar{x}_L')U'_{L_p}U_{A_m}(\bar{x}_i')U_{L_p}(x_{L_j})}{m_A(\omega^2_{A_{mp}} - \omega^2 + 2j\zeta_{A_{mp}}\omega_{A_{mp}}\omega)\left(\int_{A_A} U^2_{mp}\,\mathrm{d}A\right)}\right]. \tag{77}$$

The receptance, $\alpha_p(L,L,\omega)$, that relates a line load to a line displacement, is

$$\alpha_p(L,L,\omega) = \alpha_{LL_p} = \sum_{m=1}^{N_m}\left[\frac{U^2_{A_m}(\bar{x}_L')U'_{L_p}}{m_A(\omega^2_{A_{mp}} - \omega^2 + 2j\zeta_{A_{mp}}\omega_{A_{mp}}\omega)\left(\int_{A_A} U^2_{mp}\,\mathrm{d}A\right)}\right]. \tag{78}$$

In a similar manner, the receptance on structure B is

$$\beta_p(L,L,\omega) = \beta_{LL_p} = \sum_{m=1}^{N_m} \left[\frac{U^2_{B_m}(\bar{x}'_L)U'_{L_p}}{m_B(\omega^2_{B_{mp}} - \omega^2 + 2j\zeta_{B_{mp}}\omega_{B_{mp}}\omega)\left(\int_{A_B} U^2_{mp}\,dA\right)} \right]. \tag{79}$$

There are N_p characteristic equations of the combined system and the pth one is

$$\alpha_{LL_p}(\omega) + \beta_{LL_p}(\omega) = 0. \tag{80}$$

When the generalized distributed receptance formulation is used, the receptances along the line junction are given by equation (67). For component, A, the receptance is a diagonal matrix, in which

$$\alpha_{ii_n} = \alpha^{(n)}_{g_{A_iA_i}}(\omega) = \sum_{m=1}^{N_m} \left\{ \frac{U'_{A_m}(\bar{x}'_i)^2 U'''_{A_n}}{m_A(\omega^2_{A_{mn}} - \omega^2 + 2j\zeta_{A_{mn}}\omega_{A_{mn}}\omega)\left(\int_{A_A} U^2_{A_{mn}}\,dA\right)} \right\} \tag{81}$$

is the nth diagonal term. Similarly, for component B, the receptance is a diagonal matrix in which

$$\beta_{ii_n} = \beta^{(n)}_{g_{A_iA_i}}(\omega) = \sum_{m=1}^{N_m} \left\{ \frac{U'_{B_m}(\bar{x}'_i)^2 U'''_{B_n}}{m_B(\omega^2_{B_{mn}} - \omega^2 + 2j\zeta_{B_{mn}}\omega_{B_{mn}}\omega)\left(\int_{A_B} U^2_{B_{mn}}\,dA\right)} \right\} \tag{82}$$

is the nth diagonal term.

The characteristic equation for the system is

$$\|[\alpha_{g_{A_iA_i}}(\omega)] + [\beta_{g_{A_iA_i}}(\omega)]\| = 0 \tag{83}$$

or

$$\|[\alpha_{ii}(\omega)] + [\beta_{ii}(\omega)]\| = 0. \tag{84}$$

Because the matrices are diagonal, equation (84) reduces to

$$\sum_{n=1}^{N_n} (\alpha_{ii_{mn}} + \beta_{ii_{mn}}) = 0. \tag{85}$$

Equation (85) produces N_n equations of the form

$$\alpha_{ii_{mn}} + \beta_{ii_{mn}} = 0. \tag{86}$$

The characteristic equation developed from the line receptance formulation, equation (80), is the same as the characteristic equation developed from the distributed receptance formulation, equation (86), when it is recognized that L in the line receptance formulation plays the same role as i in the distributed receptance formulation, and that the definition of U'_{L_n} in the line receptance formulation is the same as the definition of U'''_{L_n} in the distributed receptance formulation.

Figure 2. One rod with area $2A$.

6. EXAMPLE PROBLEMS FEATURING DISTRIBUTED CONNECTIONS

The application of distributed receptances will be demonstrated by using rod problems. The rod problems were selected since corresponding analytical solutions were also available. Since the modal form of the distributed receptance is used, the problems involve the use of the distributed receptances in connection with two modal systems coupled through a distributed junction and, as such, demonstrate much of the complexity of joining complex structures.

6.2. TWO IDENTICAL RODS JOINED ALONG THEIR LENGTH

The receptance matrix for longitudinal vibration of a rod is [1]

$$[\alpha] = \begin{bmatrix} \alpha_{11} & \alpha_{12} \\ \alpha_{21} & \alpha_{22} \end{bmatrix} = -\frac{1}{kEA\sin kL}\begin{bmatrix} \cos kL & 1 \\ 1 & \cos kL \end{bmatrix}, \tag{87}$$

and thus the drive-point receptance for longitudinal vibration of a rod of length L, area A, Young's modulus E and density ρ is

$$\alpha_{11} = -\frac{\cos kL}{kEA\sin kL} = \frac{2}{\rho AL}\left[-\frac{1}{2\omega^2} + \sum_{n=1}^{\infty}\frac{1}{\omega_n^2 - \omega^2}\right], \tag{88}$$

where $k = \omega\sqrt{\rho A/EA}$ is the wavenumber of longitudinal wave propagation in the rod and $\omega_n = (n\pi/L)\sqrt{EA/\rho A}$ is the nth natural frequency of the rod. The rod in Figure 2, with length L, area $2A$, Young's modulus E and density ρ, has a drive-point receptance of

$$\gamma_{11} = -\frac{\cos kL}{2kEA\sin kL} = \tfrac{1}{2}\alpha_{11} \tag{89}$$

and thus the displacement response at node 1, due to an applied force F at node 1 is

$$u_1 = \gamma_{11}F = \tfrac{1}{2}\alpha_{11}F. \tag{90}$$

If the single rod in Figure 2 is separated into two identical rods, each with area A, joined along their lengths as in Figure 3, the line receptance formulation may be used to find the displacement response u_1 due to the force F. The receptance equations for the identical, line-connected rods are

$$u_1 = \alpha_{11}F + \bar{\alpha}_{12}^{\mathrm{T}}\bar{F}_{\alpha 2}, \qquad \bar{u}_{\alpha 2} = \bar{\alpha}_{21}F + [\alpha_{22}]\bar{F}_{\alpha 2}, \qquad \bar{u}_{\beta 2} = [\beta_{22}]\bar{F}_{\beta 2}. \tag{91–93}$$

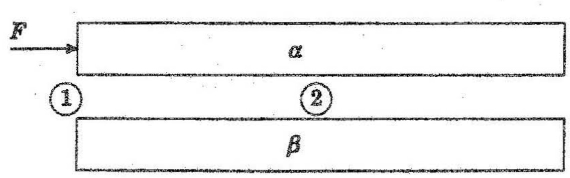

Figure 3. Two identical rods joined along their length.

By applying the force and displacement compatibility boundary conditions,

$$\bar{u}_{\alpha 2} = \bar{u}_{\beta 2}, \qquad \bar{F}_{\alpha 2} + \bar{F}_{\beta 2} = \bar{0}. \tag{94,95}$$

the force vector acting on component β is found to be

$$\bar{F}_{\beta 2} = [\alpha_{22} + \beta_{22}]^{-1}\bar{\alpha}_{21}F. \tag{96}$$

By substituting the interface force into equation (91), the drive-point displacement is found to be

$$u_1 = \alpha_{11}F - \bar{\alpha}_{12}^{T}[\alpha_{22} + \beta_{22}]^{-1}\bar{\alpha}_{21}F. \tag{97}$$

At node 2, the nth component of the generalized receptance that relates a distributed force to a distributed displacement in modal form is given by equation (64). If the modal damping assumption is replaced by a structural damping that allows the damping to be applied by means of a complex Young's modulus, i.e.,

$$E = E(1 + \mathrm{j}\eta), \tag{98}$$

where $\mathrm{j} = \sqrt{-1}$, equation (64) becomes

$$[\alpha_{g_{A_2A_2}}(\omega)] = \left[[\Phi_i]^{-1}\sum_{n=1}^{\infty}\frac{\bar{\Phi}_i\bar{\Phi}_i^{T}}{\rho A(\omega_n^2 - \omega^2)\left(\int_A U_n^2\,\mathrm{d}A\right)}\right]. \tag{99}$$

The other distributed receptances are found from equations (40) and (42). The free–free mode shapes of each of the rods is given by

$$U_n(x) = \cos((n\pi/L)x). \tag{100}$$

Since both rods have the same natural frequencies, the generalized receptance is in the same form as the line receptance that has been used primarily by Soedel [2]. In the line receptance formulation, the shape functions are selected to be the same as the mode shapes; i.e.,

$$\phi_n(x) = \cos((n\pi/L)x). \tag{101}$$

Thus, the mnth component of the distributed receptance along node 2, equation (99), becomes

$$\alpha_{g_{A_2A_2}}^{(mn)}(\omega) = \begin{cases} \dfrac{1}{\rho A(\omega_m^2 - \omega^2)}, & \text{for } m = n, \\ 0, & \text{for } m \neq n. \end{cases} \tag{102}$$

The mth component of the distributed receptances that relate nodes 1 and 2 is given by

$$\alpha_{g_{1A_2}}^{(m)}(\omega) = \frac{1}{\rho A(\omega_m^2 - \omega^2)} \tag{103}$$

and

$$\alpha_{g_{A_21}}^{(m)}(\omega) = \begin{cases} \dfrac{1}{\rho AL(-\omega^2)}, & \text{for } m = 0, \\ \dfrac{2}{\rho AL(\omega_m^2 - \omega^2)}, & \text{for } m \neq 0. \end{cases} \tag{104}$$

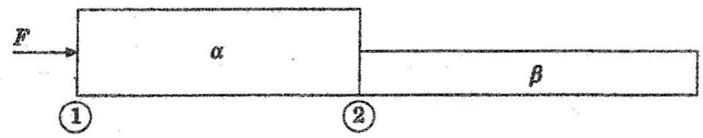

Figure 4. The two-rod receptance problem: the configuration with a point junction.

In addition, since the rod β is identical to rod α,

$$\beta^{(mn)}_{g_{A_2 A_2}}(\omega) = \alpha^{(mn)}_{g_{A_2 A_2}}(\omega) = \begin{cases} \dfrac{1}{\rho A(\omega_m^2 - \omega^2)}, & \text{for } m = n, \\ 0, & \text{for } m \neq n, \end{cases} \tag{105}$$

where

$$\omega_m = (m\pi/L)\sqrt{EA/\rho A}. \tag{106}$$

Substitution of equations (102), (103), (104) and (105) into the last term of equation (97) gives

$$\bar{\alpha}^{T}_{12}[\alpha_{22} + \beta_{22}]^{-1}\bar{\alpha}_{21}F = \frac{F}{2}\sum_{m=0}^{\infty} \alpha^{(m)}_{g_{A_2 1}}(\omega)$$

$$= \frac{F}{\rho AL}\left[\frac{1}{-\omega^2} + \sum_{m=1}^{\infty}\frac{1}{\omega_m^2 - \omega^2}\right] = -\frac{F}{2}\alpha_{11} \tag{107}$$

and equation (97) becomes

$$u_1 = \tfrac{1}{2}\alpha_{11}F, \tag{108}$$

which is the same as the result given in equation (90) for the receptance of a rod having twice the area of the individual component rods. Thus the distributed receptance (and line receptance) formulation gives a result identical to the analytical solution predicted by using the point-to-point receptance. In this case the distributed receptance formulation provided an exact solution for the response of the rod having twice the area, since the series of shape functions was not truncated. In practice, when more complicated structures are joined the series will need to be truncated and the results will only approximate the exact analytical solution. The accuracy of the approximation will be governed by how well the displacement response of the interface can be represented by the shape functions, ϕ_n.

6.2. TWO RODS OF DIFFERENT LENGTHS JOINED ALONG THEIR LENGTH

Although the above example involved a simple problem, equation (97) represents the drive-point displacement of any two-component system. By connecting a rod having area A to the end of the rod considered in the first example, one obtains the geometry shown in Figure 4. The displacement at node 1 in Figure 4 may be found from equation (97) to be

$$u_1 = \left(\alpha_{11}F - \frac{\alpha_{12}\alpha_{21}}{(\alpha_{22} + \beta_{22})}\right)F, \tag{109}$$

where the receptances are given by

$$\alpha_{11} = \alpha_{22} = -\frac{\cos kL}{2kEA\sin kL}, \qquad \alpha_{12} = \alpha_{12} = -\frac{1}{2kEA\sin kL} \tag{110,111}$$

and

$$\beta_{22} = -\frac{\cos kL}{kEA\sin kL}, \tag{112}$$

where

$$k = \omega\sqrt{\rho A/EA}. \tag{113}$$

By substituting equations (110), (111) and (112) into equation (109), the displacement response at node 1 is found to be

$$u_1 = \frac{(1 - 3\cos^2 kL)}{6kEA\sin kL\cos kL}F. \tag{114}$$

The same problem can be represented differently, however, For example, in Figure 5 the problem is represented such that rod α of length L and area A, and rod β of length $2L$ and area A, are joined along a distributed line-connection at node 2. The displacement response at node 1 is then given by equation (97), where

$$\alpha_{11} = -\frac{\cos kL}{kEA\sin kL} = \frac{2}{\rho AL}\left[-\frac{1}{2\omega^2} + \sum_{n=1}^{\infty}\frac{1}{\omega_n^2 - \omega^2}\right], \tag{115}$$

and the distributed receptances are defined by equations (40), (41) and (42). Rod α is the same as the rod α that was considered in the line receptance example above. Thus, when the same shape functions, $\cos(n\pi x/L)$, are used, the distributed receptances for rod α are given by equations (102), (104) and (103), where

$$\omega_m = (m\pi/L)\sqrt{EA/\rho A}. \tag{116}$$

The distributed receptance of rod β at node 2 is obtained from equation (42) and can be rewritten as

$$[\beta_{22}(\omega)] = \left[\int_0^L \bar{\phi}(\bar{x})\bar{\phi}(\bar{x})^{\mathrm{T}}\mathrm{d}x\right]^{-1} \sum_{m=1}^{N_m} \frac{\left\{\int_0^L U_m^{\beta}(x)\bar{\phi}(x)\mathrm{d}x\right\}\left\{\int_0^L U_m(x)\bar{\psi}(x)\mathrm{d}x\right\}^{\mathrm{T}}}{\rho A(\omega_m^{\beta 2} - \omega^2)\left(\int_0^{2L} U_m^{\beta 2}\mathrm{d}x\right)}, \tag{117}$$

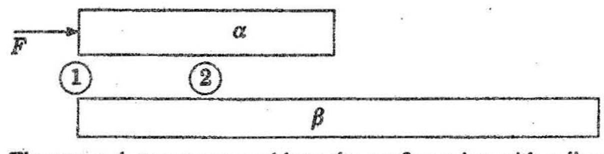

Figure 5. The two-rod receptance problem: the configuration with a line junction.

$$U_m^\beta = \cos((m\pi/2L)x), \qquad \omega_m^\beta = \frac{m\pi}{2L}\sqrt{\frac{EA}{\rho A}}. \tag{118,119}$$

After substituting

$$\phi_m(x) = \cos((m\pi/L)x) \tag{120}$$

into equation (117), the receptance of rod β is found to be

$$[\beta_{22}(\omega)] = \frac{2}{\rho A L^2}\begin{bmatrix} \frac{1}{2} & 0 & 0 & \\ 0 & 1 & 0 & \\ 0 & 0 & 1 & \\ & & & \ddots \end{bmatrix} \left[\frac{1}{2}\frac{IL_{0\bar{m}}IL_{0\bar{n}}{}^{\mathrm{T}}}{\omega_0^{\beta^2} - \omega^2} + \sum_{p=1}^{N_p}\frac{IL_{p\bar{m}}IL_{p\bar{n}}{}^{\mathrm{T}}}{\omega_p^{\beta^2} - \omega^2}\right], \tag{121}$$

where

$$IL_{p\bar{n}} = \int_0^L \cos\left(\frac{p\pi}{2L}x\right)\cos\left(\frac{\bar{n}\pi}{L}x\right)\mathrm{d}x = \frac{L}{2}\left(\mathrm{sinc}\left(\frac{p}{2}+\bar{n}\right) + \mathrm{sinc}\left(\frac{p}{2}-\bar{n}\right)\right), \tag{122,123}$$

$$\mathrm{sinc}(x) = \frac{\sin(\pi x)}{\pi x}, \qquad \bar{m} = \begin{Bmatrix} 1 \\ 2 \\ \vdots \\ N_m \end{Bmatrix}, \quad \bar{n} = \begin{Bmatrix} 1 \\ 2 \\ \vdots \\ N_n \end{Bmatrix}. \tag{124–126}$$

By substituting the receptances defined in equations (102), (103), (104) and (121) into equation (97), the displacement response of the system shown in Figure 5 may be found. For the purpose of calculation, the rods shown in Figure 5 were assumed to have a Young's modulus E of $19{\cdot}5 \times 10^{10}\,\mathrm{N/m^2}$, a density ρ of $7700\,\mathrm{kg/m^3}$, a damping factor η of 0·01, an area A of $1{\cdot}0 \times 10^{-4}\,\mathrm{m^2}$ and a length L of 0·5m. A comparison of the displacement response found using the distributed receptance model, and the displacement response found using the point receptance model shown in Figure 4, is presented in Figure 6. The distributed receptance formulation provides good results and converges towards the point receptance prediction as the number of modes (and hence shape functions) is increased. Note that for the sake of simplicity, the number of modes used to predict the modal response was made equal to the number of shape functions used to fit the interaction along node 2.

A case having identical material and geometrical values except that the second rod was assumed to be only $1{\cdot}8L$ in length was also analyzed. In the point-connected case, the only change is that β_{22} is now given by

$$\beta_{22} = -\frac{\cos(0{\cdot}8\mathrm{kL})}{kEA\sin(0.8kL)}. \tag{127}$$

In the distributed receptance case, $[\beta_{22}]$ becomes

$$[\beta_{22}(\omega)] = \frac{2}{0{\cdot}9\rho A L^2}\begin{bmatrix} \frac{1}{2} & 0 & 0 \\ 0 & 1 & 0 \\ 0 & 0 & 1 \\ & & \end{bmatrix} \left[\frac{1}{2}\frac{IL_{0\bar{m}}IL_{0\bar{n}}{}^{\mathrm{T}}}{\omega_0^{\beta^2} - \omega^2} + \sum_{p=1}^{N_p}\frac{IL_{(p/0\cdot9)\bar{m}}IL_{(p/0\cdot9)\bar{n}}{}^{\mathrm{T}}}{\omega_p'^{\beta^2} - \omega^2}\right], \tag{128}$$

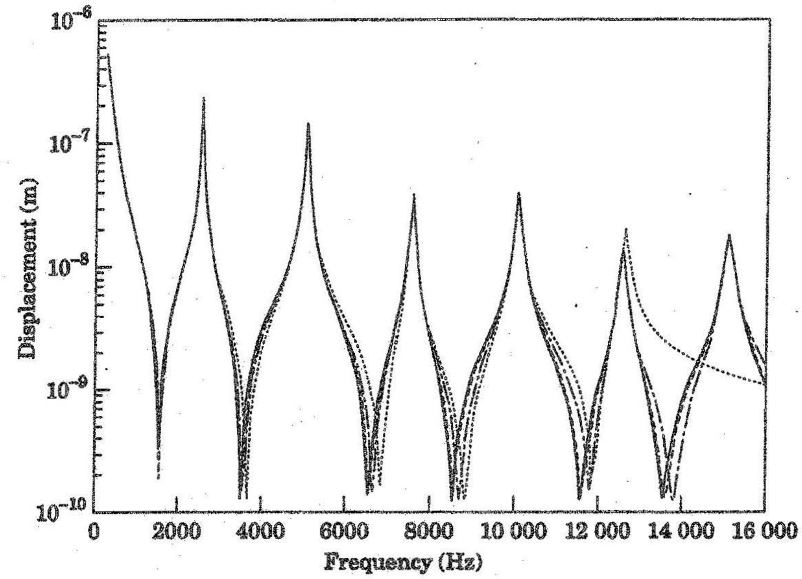

Figure 6. The displacement response of two rods with different lengths (L and $2L$) joined along their length. ——, Point receptance; ···, distributed receptance with five modes; –·–, distributed receptance with ten modes.

In the distributed receptance case, $[\beta_{22}]$ becomes

$$[\beta_{22}(\omega)] = \frac{2}{0\cdot 9\rho AL^2}\begin{bmatrix}\frac{1}{2}&0&0&\\0&1&0&\\0&0&1&\\&&&\ddots\end{bmatrix}\left[\frac{1}{2}\frac{IL_{0\hat{n}}IL_{0\hat{n}}^{T}}{\omega_0^{\beta 2}-\omega^2}+\sum_{p=1}^{N_p}\frac{IL_{(p/0\cdot 9)\hat{n}}IL_{(p/0\cdot 9)\hat{n}}^{T}}{\omega_p'^{\beta 2}-\omega^2}\right], \qquad (128)$$

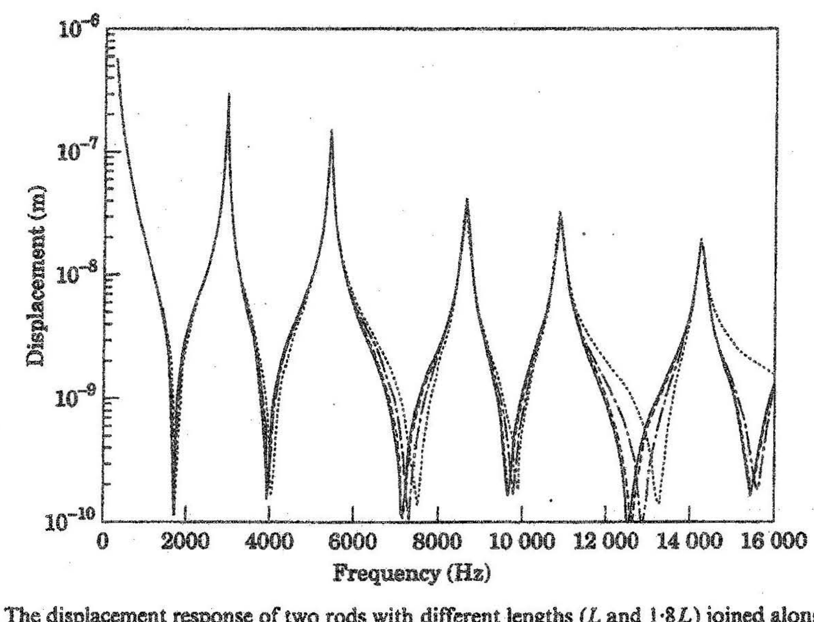

Figure 7. The displacement response of two rods with different lengths (L and $1\cdot 8L$) joined along their length. ——, Point receptance; ···, distributed receptance with five modes; –·–, distributed receptance with ten modes.

where

$$\omega_m'^{\beta} = (m\pi/1{\cdot}8L)\sqrt{EA/\rho A}. \tag{129}$$

The displacement response found using the distributed receptance model and the displacement response found by using the point receptance model are compared in Figure 7: again, good agreement and convergence were obtained. Thus, in the case in which the lengths of the two rods are not integer multiples, the distributed receptance formulation still provides good results and converges towards the correct response as the number of modes (and shape functions) is increased. It appears that the convergence rate is slightly faster when the lengths of the rods are integer multiples. However, further work would be required to draw a firm conclusion in this respect.

7. CONCLUSIONS

In this paper, the receptance matrix formalism has been extended to accommodate distributed connections between components. In particular, the extension was based on generalized Fourier series concepts. The receptances for distributed connections were shown to reduce to the previously developed line receptance formulation in problems for which the latter approach is appropriate. The performance of the distributed receptance method was demonstrated through two example problems involving rods. The capabilities of the distributed receptance method presented here should make it possible to automate the development of analytically based models of complex structures more easily, thus making them accessible to a wider audience of structural analysts.

The receptance method can be used to solve both free and forced vibration problems. Traditionally, some of the advantages of the receptance method are: (i) that it is well suited to cases in which experimental and analytical data are mixed; (ii) that it is particularly useful for analyzing systems made up of a small number of components; and (iii) that it often provides better insight into the physical mechanisms behind a response than other numerical methods. The receptance method had been improved by Jetmundsen *et al.* [12] and Gordis *et al.* [13] to allow automated assembly of the system receptance matrix. That modification allows the receptance method to be used as a general purpose analysis tool, much like the finite element method. With the addition here of the ability to model arbitrary distributed junctions, the receptance method now provides a potential alternative to finite element analysis.

Some of the advantages of a receptance element method over the finite element method are the ability to seamlessly mix analytical, modal, numerical and experimental receptances, and the potential to use larger analytical elements. In addition, it should be more straightforward to update models with experimental data than it is when using finite elements. Note, however, that the use of distributed receptances will be limited by: (i) the difficulty in obtaining a closed form Green function for plates and shells having arbitrary boundary conditions; (ii) the non-linearity of the eigenvalue problem that requires a determinant search; and (iii) the lack of readily available algorithms for assembling the system receptance matrix. The lack of a closed form Green function in many cases may be overcome by use of a modal model of the system. When using a modal description of the component receptances, the receptance method becomes an alternative component mode synthesis method.

REFERENCES

1. R. E. D. Bishop and D. C. Johnson 1960 *The Mechanics of Vibration*. London: Cambridge University Press.

2. W. Soedel 1993 *Vibrations of Shells and Plates*. New York: Dekker.
3. I. D. Wilken and W. Soedel 1976 *Journal of Sound and Vibration* **44**, 563–576. The receptance method applied to ring-stiffened cylindrical shells: analysis of modal characteristics.
4. I. D. Wilken and W. Soedel 1976 *Journal of Sound and Vibration* **44**, 577–589. Simplified prediction of the modal characteristics of ring-stiffened cylindrical shells.
5. D. T. Huang 1991 *Ph.D. Thesis, School of Mechanical Engineering, Purdue University*. On the free and forced vibrations of plate–shell combinations using the receptance method.
6. D. T. Huang and W. Soedel 1993 *Journal of Sound and Vibration* **166**, 315–339. On the free vibrations of multiple plates welded to a cylindrical shell with special attention to mode pairs.
7. S. Azimi, J. F. Hamilton and W. Soedel 1984 *Journal of Sound and Vibration* **93**, 9–29. The receptance method applied to the free vibration of continuous rectangular plates.
8. S. Azimi, W. Soedel and J. F. Hamilton 1986 *Journal of Sound and Vibration* **109**, 79–88. Natural frequencies and modes of cylindrical polygonal ducts using receptance methods.
9. W. Soedel 1987 *Journal of Sound and Vibration* **115**, 365–366. Reply by one of the authors.
10. J. M. Cuschieri 1990 *Journal of the Acoustical Society of America* **87**, 1159–1165. Structural power-flow analysis using a mobility approach of an L-shaped plate.
11. D. T. Huang and W. Soedel 1993 *Journal of Sound and Vibration* **166**, 341–369. Study of the forced vibration of shell–plate combinations using the receptance method.
12. B. Jetmundsen, R. L. Bielawa and W. G. Flannelly 1988 *Journal of the American Helicopter Society* **33**, 55–64. Generalized frequency domain substructre synthesis.
13. J. H. Gordis, R. L. Bielawa and W. G. Flannelly 1991 *Journal of Sound and Vibration* **150**, 139–158. A general theory for frequency domain structural synthesis.
14. J. W. Nicholson 1986 *American Institute of Aeronautics and Astronautics* **24**, 485–491. Free vibration of stiffened rectangular plates using Green's functions and integral equations.
15. K. Kelkel 1987 *American Institute of Aeronautics and Astronautics* **25**, 1482–1489. Green's function and receptance for structures consisting of beams and plates.
16. D. J. Gorman 1982 *Free Vibration Analysis of Rectangular Plates*. New York: Elsevier.
17. J. O. Hallquist and V. W. Snyder 1974 *Journal of Sound and Vibration* **32**, 131–142. On the connection of viscously damped continuous vibratory systems.
18. J. Tzioufas, D. M. McFarland and L. A. Bergman 1994 *Journal of Sound and Vibration* **174**, 1–22. Vibration of multiple-point connected discrete-distributed structures.
19. A. V. Pesterev and G. A. Tavrizov 1994 *Journal of Analytical and Experimental Modal Analysis* **9**, 302–316. Structural analysis method for dynamic analysis of conservative structures.
20. S. A. Hambric 1994 *ASME Technical Report* 94-WA/NCA-9. Approximation techniques for broad-band acoustic radiated noise design optimization problems.
21. B. K. Gardner 1995 *Ph.D. Thesis, School of Mechanical Engineering, Purdue University*. External system modeling with application to vibro-acoustic optimization.
22. R. V. Churchill 1987 *Fourier Series and Boundary Value Problems*. New York: McGraw-Hill; fourth edition.